Welding of Galvanized Dual-Phase 980 Steel in a Gap-Free Lap Joint Configuration

A new welding procedure based on GTAW as an auxiliary preheating source with a fiber laser as a main heat source has been developed to obtain the completely defect-free lap joints of galvanized DP 980 steel in a gap-free configuration

BY S. L. YANG AND R. KOVACEVIC

ABSTRACT

The feasibility has been investigated of producing sound gap-free lap joints in galvanized DP980 steel with laser beam welding and hybrid laser-gas tungsten arc welding (GTAW) with a common molten pool. Laser-welded lap joints and hybrid laser-GTA welded lap joints were characterized by different weld defects such as spatters and blowholes. A new welding procedure based on using GTAW as an auxiliary preheating source with a fiber laser as a main heat source is proposed to join the galvanized DP 980 steel in a gap-free lap joint configuration. The metal oxides produced during the GTAW preheating process can drastically improve the coupling of the laser beam to the welded material. Under this welding condition, the keyhole is readily formed by the laser beam and provides the channel for the highly pressurized zinc vapor developed at the interface of two metal sheets during the laser welding process to be vented out. The completely defect-free laser welds have been obtained by using this newly developed welding method. X-ray photoelectron spectroscopy (XPS) test is carried out to analyze the chemical compositions of the surface preheated by the GTAW torch. A CCD video camera with the frame rate of 30 frames per second is used to monitor the molten pool online. Microhardness measurement, SEM microstructure analysis, as well as a tensile-shear test were carried out to evaluate the mechanical properties of the hybrid GTAW preheated/laser welded joints with the separate molten pool.

S. L. YANG (shangluy@smu.edu) is a PhD candidate and R. KOVACEVIC (kovacevi@lyle.smu.edu) is director of the Center for Advanced Manufacturing and NSF I/UCRC Center for Laser-Aided Manufacturing, Southern Methodist University, Dallas, Tex.

Introduction

Because of their excellent corrosive resistance, galvanized steels have been widely used in different industries such as automotive and shipbuilding. However, it is still a great challenge to weld the galvanized steels in a gap-free lap joint configuration. Due to the low boiling point of zinc (906°C) with respect to the melting point of steels (over 1500°C), the highly pressurized zinc vapor is easily developed at the interface of the two metal sheets. The highly pressurized zinc vapor expels the liquid metal out of the molten pool and produces different defects in the weld such as spatter and porosity. These weld defects significantly degrade the mechanical properties of the welded joints.

In order to mitigate the presence of the highly pressurized zinc vapor when using a laser beam to join the galvanized steels, a number of welding procedures have been developed in the past several decades. The simplest approach to mitigate the effect of the zinc vapor is to completely remove the zinc coating at the interface by mechanical means prior to welding (Ref. 1), as one of the American Welding Society standards for welding galvanized steel suggested (Ref. 2). Another technique used to weld lap joints in galvanized steels is to intentionally form a small root opening between the two metal sheets (Ref. 3). Mazumder et al. (Ref. 4) patented and described (Refs. 5, 6) a technique that places a thin copper sheet between two steel sheets along the weld interface. The copper has a melting temperature of 1083°C (between the melting temperatures of steel and the boiling temperature of zinc) and can be alloyed with the zinc before the steel is melted. However, the presence of copper in the steel could generate additional problems, such as hot cracking and corrosion concerns (Ref. 7). The method of redesigning the lap joint, which allows the zinc vapor to be evacuated before the molten pool reaches the interface, is another way of mitigating the effect of the zinc vapor (Refs. 8–11). Pennington et al. (Refs. 12, 13) replaced the zinc coating in the weld zone with a nickel coating before laser welding; the nickel coating's melting point of 1453°C is higher than the melting point of zinc. By replacing the zinc coating with nickel coating in the weld area, the welding process is not affected by the highly pressurized zinc vapor and corrosion protection is still provided. However, this will increase the cost and lower the productivity. In addition, pulsed laser (Ref. 14), dual laser beam or two lasers (Refs. 15–19), and hybrid laser welding (Refs. 20–23) were also applied to lap join the galvanized steels. Gualini et al. (Ref. 18) proposed the modified dual-beam method to weld galvanized steel sheets in a gap-free lap joint configuration. In their studies, the first beam was used to cut a slot, which provided an exit path for the zinc vapor, while the second beam was employed to join the metal sheets. However, it was found that spatter and porosity were still produced in the welds by using this method. Kim et al. (Ref. 23) used the laser-arc hybrid welding technique to join 1.0-mm-thick SGCD1 galvanized low-strength steel in a gap-free lap joint configuration. They found that the formation of porosity was the main concern in the welding of galvanized steels. Moreover, the welding process is not stable in their study. Spatter and porosity are still produced in the welds, which significantly damages the electrode torch and lowers the mechanical properties of the welds. Additionally, Gu et al. (Ref. 24) also introduced the arc to share a common molten pool with the laser welding process, in which the molten pool is enlarged by the arc. The enlarged pool can provide more space for the zinc vapor to es-

KEYWORDS

Galvanized Steels
Hybrid Laser/GTA Welding
Metal Oxides
X-Ray Photoelectron Spectroscopy
CCD Video Camera
Keyhole

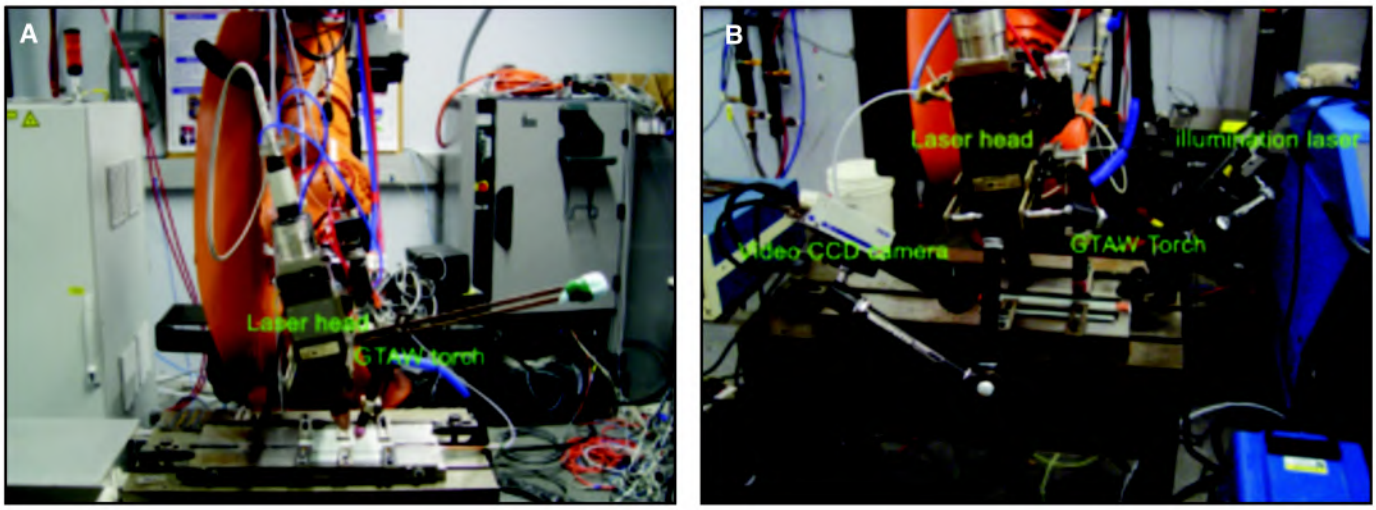

Fig. 1 — A — Experimental setup for hybrid laser/GTA welding in the common molten pool; B — experimental setup for hybrid GTAW preheating/laser welding in a separated molten pool.

cape from it. However, spatter and porosity were present in the welds. Recently, Li et al. (Ref. 25) patented and described in a paper (Ref. 26) a technique that sets the aluminum foil layer in the weld zone at the interface of two galvanized steel sheets to form the Al-Zn alloy; thus lowering the effect of the zinc vapor pressure. In order to use this method to weld galvanized steels in a lap configuration, there is a requirement of tightly clamping the two metal sheets. If a gap exists at the interface of two metal sheets, weld defects will form (Ref. 26). Furthermore, the dissolution of aluminum-steel alloy into the weld, which makes the weld brittle, has the potential to deteriorate the weld quality. Although the methods mentioned here can mitigate the presence of the highly pressurized zinc vapor at the interface of two metal sheets, they also have a number of disadvantages. Some of the proposed methods require preprocessing or postprocessing actions. Some require a high investment in equipment. In addition, during laser welding of steel, the coupling efficiency of laser beam energy is very low (Ref. 27). It has been reported that different surface conditions could affect the absorbability of the laser beam energy by the metal sheets (Refs. 28, 29).

Dual-phase steels offer low yield ratio, high work-hardening ratio, and high bake hardening (BH) value. They have been used to manufacture auto components that demand high strength and good "crashworthiness and formability" such as "wheel, bumper, and other reinforcements" (Ref. 30). According to the UltraLight Steel Auto Body (ULSAB) program report, 74% of the ULSAB body structure is constructed of dual-phase steels (Ref. 31).The automotive industry has shown considerable interest in using laser welding techniques for replacing traditional spot welding to lap join galvanized dual-phase steels in a gap-free configuration. Because of its high speed, low heat input, and low distortion, laser beam welding has been widely used in the automotive industry to fabricate different vehicles parts (Refs. 32, 33). While the automotive industry has shown significant interest in using laser welding techniques to lap join galvanized DP steels in a gap-free configuration, until now there has been no report on a cost-effective, efficient, and easy-to-use laser welding technique that can be practically applied to do so. To meet the requirement of obtaining sound lap joints for the automotive industry, therefore, it is important to develop an efficient and robust laser welding technique for welding of galvanized steels in a gap-free lap joint configuration and to fully understand the mechanisms of the welding process. The main objective of this study is focused on developing a welding procedure to provide completely defect-free, gap-free lap joints in galvanized DP steels for the automotive industry.

In this study, laser welding is first used to weld galvanized DP980 steel metal sheets in a gap-free lap joint configuration. A large amount of spatter and porosity are produced during the laser welding process. Furthermore, in order to mitigate the presence of zinc vapor developed at the interface of two metal sheets, gas tungsten arc welding (GTAW) is combined with fiber laser welding in two modes to weld galvanized dual-phase DP 980 steel in a gap-free lap joint configuration. In the first mode, the laser beam and GTAW share a common molten pool. This approach was taken by other re-

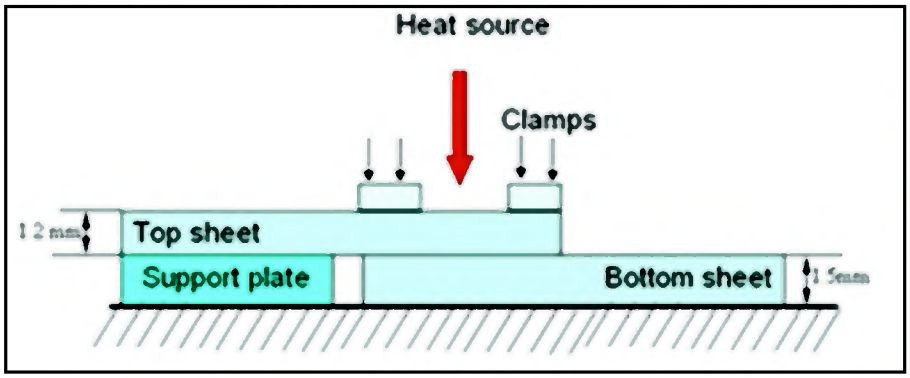

Fig. 2 — Schematic representation of the setup of gap-free lap joint configuration for the hybrid laser-GTAW preheating process.

Fig. 3 — Typical laser beam welded lap joint (laser power: 3000 W and welding speed of 30 mm/s).

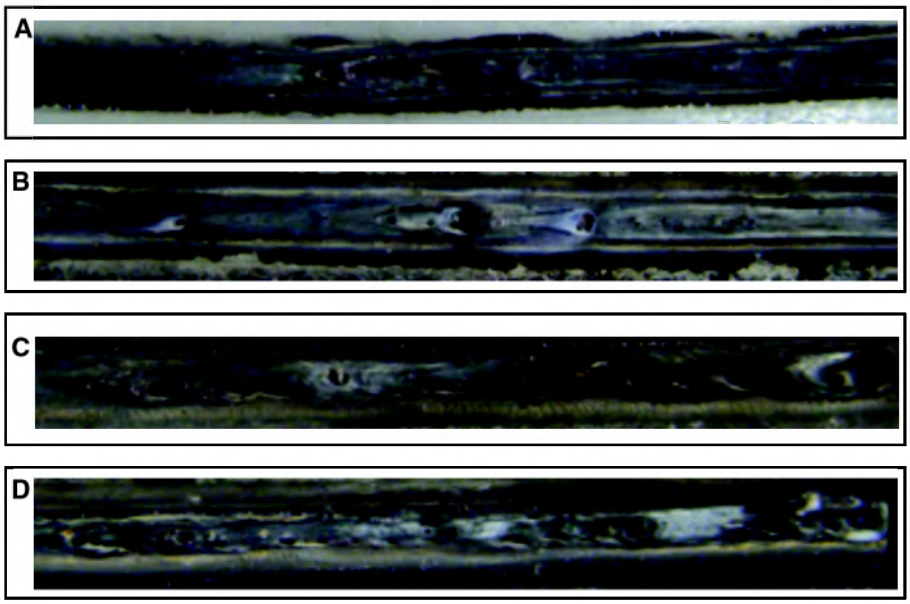

Fig. 4 — The effect of laser power on weldability using hybrid laser/GTAW in a common molten pool at the following laser powers: A — 2000 W; B — 2500 W; C — 3000 W; D — 3500 W. (Arc current: 200 A and welding speed: 30 mm/s.)

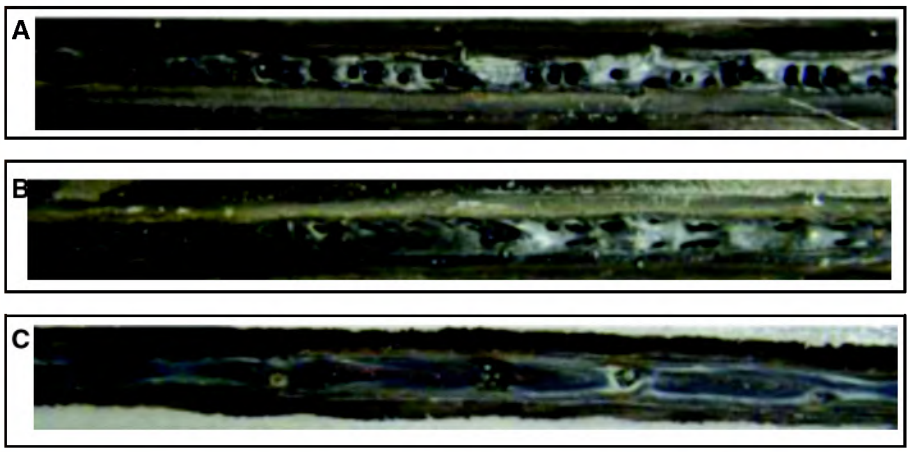

Fig. 5 — The effect of the distance between the GTAW electrode and the laser beam using hybrid laser/GTAW in a common molten pool at the following distances: A — 2 mm; B — 6 mm; C — 10 mm. (Laser power: 3000 W, arc current: 200 A, and welding speed: 30 mm/s.)

searchers (Refs. 23, 24). The effects of welding parameters on the feasibility of producing joints in a gap-free lap joint configuration are fully investigated. In the second mode, GTAW is only used as the preheating source to modify the surface conditions of the top surface in order to improve the coupling efficiency of the laser beam energy with the metal. In this approach, the laser beam and GTAW torch are kept at a specific distance. Through the controlled heat management of GTAW preheating process, the zinc coating at the top surface of the metal sheet is burned and metal oxides are generated at the top surface along the weld interface. In addition, the zinc coating along the weld interface of two metal sheets is transformed in the zinc oxides, and has a higher melting point (1975°C) than the boiling point of zinc (906°C). The following laser beam is used to provide the required depth of weld penetration. Completely defect-free laser welds have been obtained using this newly developed welding method. Additionally, a CCD video camera with the frame rate of 30 frames per second was used to monitor the molten pool behavior online. It was found that the keyhole is the critical factor to guarantee successful achievement of defect-free galvanized DP 980 steel lap joints. X-ray photoelectron spectroscopy (XPS) tests were carried out to determine the chemical composition at the top surface as well as along the interface of the metal sheets. The microhardness and test tensile shear tests are carried out to evaluate mechanical properties of the welds. The microstructures in the different zones of welds are analyzed by using a scanning electron microscope (SEM). It was found that the decrease in the volume of the martensite in the heat-affected zone (HAZ) reflected into the decrease in the hardness value in the HAZ. The tensile shear test results show that the fracture of welds mainly occurred in the HAZ.

Experimental Setup

The material used in this study is galvanized DP 980 steel sheet. The dimensions of the coupons used in this study are 200 × 85 × 1.2 mm and 200 × 85 × 1.5 mm. The 1.2-mm-thick coupon is selected to be at the top of the lap joint welding process. The gap between the two metal sheets is kept tight during welding, assuming that the gap is equal to zero. The laser/GTAW hybrid welding experiments are performed by using a 4-kW fiber laser, which has a 250-mm focal length and a 0.6-mm focused spot size. The GTAW machine is a 300 DX AC/DC inverter argon arc welding machine. Pure argon gas with the flow rate of 30 ft^3/min is used as the shielding gas. A 3-mm-diameter GTAW electrode is used. A CCD color video camera is used to monitor the welding process. The video frame rate is set at 30 interlaced frames per second. A bandpass green laser with a 532-nm center wavelength and a maximum output power of 6 W is selected as the source to illuminate the molten pool in order to obtain clear images of it. The experimental setup is shown in Fig. 1. During the welding process, hybrid laser/GTAW is performed in two modes: in the first mode, the laser beam and GTAW torch share the common molten pool; and in the other, the laser beam and GTAW torch are kept at the appropriate distance. Welding is performed with the laser head tilted at 10 deg from the normal to the sheet surface in order to prevent the reflected laser light and the spatter from damaging the laser optics, as shown in Fig. 1. The GTAW torch is kept in the vertical position. Table 1 lists the chemical compositions of the galvanized DP 980 steels. Figure 2 shows the schematic presentation of the gap-free lap joint configuration for hybrid laser/GTA welding.

Results and Discussion

Laser Welding of Galvanized Dual-Phase DP 980 Steel in a Gap-Free Lap Joint Configuration

In order to investigate the influence of different welding parameters on the weld quality of laser-welded lap joints, laser power and welding speed are varied and a thin foil of stainless steel in thicknesses of 0.1, 0.2, and 0.4 mm is set as the gap in the weld zone to weld dual-phase DP 980 steels in a gap-free lap joint configuration. Figure 3 illustrates the typical surface appearance of a gap-free lap joint of galvanized DP 980 steel using laser welding. As shown in Fig. 3,

the laser-welded galvanized DP 980 steel joint is characterized by the presence of spatter and porosity, which are produced by the highly pressurized zinc vapor developed at the interface. When using the laser welding to join the galvanized steels in the gap-free configuration, it is difficult to safely vent out the highly pressurized zinc vapor from the small molten pool the laser beam produces. The highly pressurized zinc vapor tends to violently expand, expel from the molten pool, and remove liquid metal out of the molten pool (Ref. 34). The liquid metal removed from the molten pool is condensed in the air and produces different-sized spatter that scatters in all directions and is deposited in and/or around the weld zone. Moreover, excessive removal of the molten material will lead to the formation of porosity (Ref. 35). From the experimental results, it could be concluded that it is impossible to obtain sound welds of galvanized DP 980 steel using only laser welding in a gap-free lap joint configuration. In addition, it is found that the laser-induced plasma directly above the top surface of metal sheets fluctuates dramatically and this irregular plasma makes coupling of the laser beam very instable.

Feasibility Study of Gap-Free Lap Joint of Galvanized DP 980 Steel Using Hybrid Laser/GTA Welding with the Common Molten Pool

In order to address the problems caused by highly pressurized zinc vapor that develops at the interface of two metal sheets, GTAW is introduced to share the common molten pool to weld galvanized DP 980 steels in a gap-free configuration. The effects of the main process parameters on the weldability of galvanized DP 980 steel such as laser power, the distance between laser beam and electrode torch, and the arc current, as well as the welding speed are studied. Figure 4 shows the effect of laser power on the feasibility of achieving sound welds. Figure 5 shows the effect of distance between the laser beam and electrode torch on the surface appearance of hybrid laser/GTA welded joints. Figure 6 shows the effect of arc current on the surface appearance of hybrid laser/GTA welded joints. Figure 7 shows the effect of welding speed on the surface appearance of hybrid laser/GTA welded joints. As shown in Fig. 4, increasing laser power produces more spatter in the welds due to the higher heat input, which increases the pressure of zinc vapor at the interface of two metal sheets and makes the welding process more unstable. The stability of the welding process is improved by the increase in the distance between the laser beam and electrode torch, as shown in Fig. 5. This phenomenon is attributed to the lowering pressure of zinc vapor with the increase in the distance between the laser beam and GTAW torch and the partially burned zinc coating at the interface by the leading arc. In addition, the leading arc also oxidized the zinc coating in and around the weld zone at the interface of the two metal sheets. The zinc oxides have a higher melting point (1975°C for ZnO) than the boiling point of zinc (906°C), thus helping to stabilize the welding process (Ref. 23). Furthermore, it was found that the increase in the specific range of arc current, as shown in Fig. 6, improved the weld quality of the galvanized DP 980 steel. This phenomenon could be explained by the fact that the size of the molten pool is enlarged by increasing the arc current. However, the weld quality of the galvanized DP 980 steel decreases with the increase in welding speed, as shown in Fig. 7. The main reason for this is the fact that the keyhole will collapse when the welding speed is increased (Ref. 36).

With respect to laser welding of galvanized DP 980 steels, the hybrid laser/GTAW process with a common molten pool will produce less spatter because the addition of the arc will enlarge the molten pool. More importantly, the arc preheats the metal

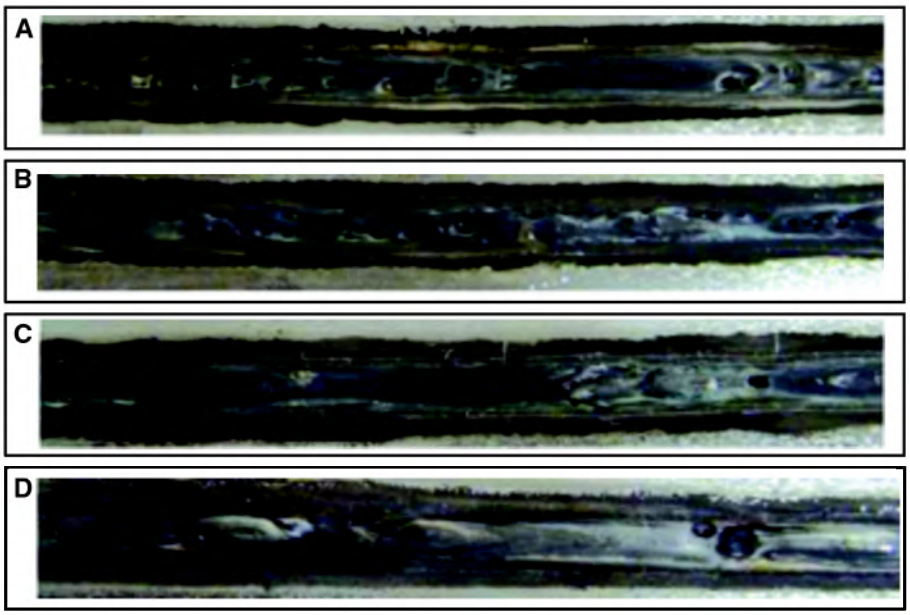

Fig. 6 — The effect of arc current using hybrid laser/GTAW in a common molten pool at the following arc currents: A — 120 A; B — 160 A; C — 200 A; D — 240 A. (Laser power: 3000 W and welding speed of 30 mm/s.)

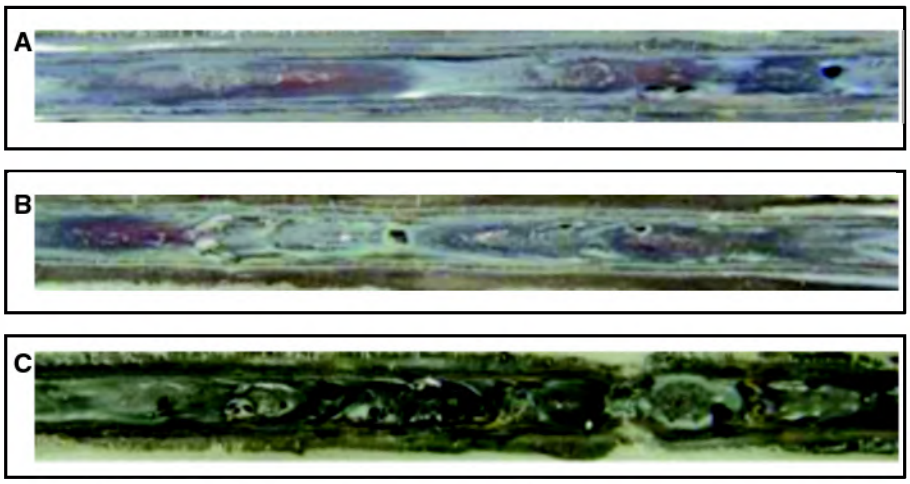

Fig. 7 — The effect of welding speed using hybrid laser/GTAW in a common molten pool at the following welding speeds: A — 30 mm/s; B — 35 mm/s; C — 40 mm/s. (Laser power: 3000 W, arc current: 200 A, and the distance between laser beam and GTAW electrode: 6 mm.)

Table 1 — Chemical Composition (wt-%) of DP 980 Steel

Steel	C	Mn	Mo	Si	Cr	Al	B
DP 980	0.135	2.1	0.35	0.05	0.15	0.45	0.007

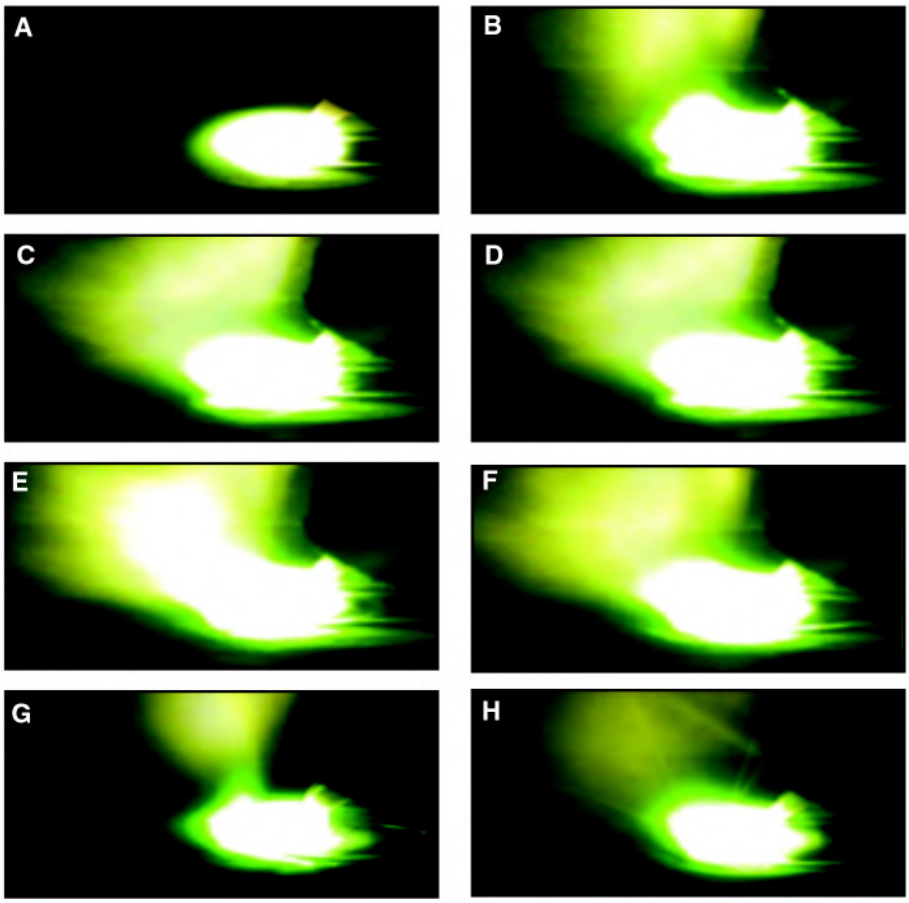

Fig. 8 — The shape of the arc plasma and the zinc vapor plume at different times: A — t = 0 ms; B — t= 30 ms; C — t = 70 ms; D — t = 100 ms; E — t = 130 ms; F — t = 170 ms; G — t = 200 ms; and H — t = 230 ms.

sheets. This facilitates the absorptivity of the laser beam into the metal sheets. The laser beam forms a hole in the molten pool, through which the zinc vapor will be vented out. However, it is still difficult to completely eliminate the generation of spatter, which tends to damage the expensive laser optical lens. In addition, spatter severely damages the electrode tip; thus, it is necessary to frequently sharpen it. Furthermore, when the laser beam and the electrode share a common molten pool, the plasma defocuses, absorbs, and refracts the laser beam (Refs. 37, 38). Figure 8 shows eight consecutive images of the interaction between the laser beam and arc taken by the video CCD camera. As shown in Fig. 8, the shapes of the arc and vapor plume vary over time. The irregular arc plasma and the metal vapor plume, especially the highly pressurized zinc vapor, leads to significant instability of the coupling of laser beam energy into the specimens; thus, the keyhole tends to collapse. As a result, the welding process becomes unstable and the keyhole tends to collapse, which in turn influences the coupling of laser beam and arc and produces lots of spatter and/or porosity in the welds.

Another issue arising from using hybrid laser/GTAW in a common molten pool to gap-free lap join the galvanized steels is the formation of porosity in the welds. As shown in Fig. 9, porosity is produced at the top surface of welds and in the internal weld fusion zone, the location of which is dependent on the welding conditions. The main reason for porosity formation is the entrapment of air and the shielding gas as well as the metal vapor into the molten pool. If these entrapped gases or metal vapors cannot escape from the molten pool during weld solidification, porosity is produced. Additionally, the collapse of the keyhole is also responsible for formation of porosity (Ref. 39). At the same time, it has been revealed that the increase in temperature exponentially increases the pressure level of the zinc vapor, as shown in Fig. 10 (Ref. 40). When the laser beam shares a common molten pool with the arc, the temperature at the interface of the two metal sheets dramatically increases due to the higher heat input; thus, the zinc vapor reaches a very high pressure level. This fact implies that the function of the arc-enlarged molten pool cannot completely compensate for the increase in the pressure level. From the further experimental results, it was found that only in a very narrow optimized welding condition can the spatter and porosity be dramatically decreased and a sound weld be obtained with the introduction of the arc. Additionally, the zinc coating at the top surface and the interface of the two metal sheets is widely damaged by the arc and the weld surface is nonuniform when the laser beam and GTAW torch share a common molten pool.

Gap-Free Lap Joint of Galvanized DP 980 Steels Using Hybrid Laser/GTA Welding with a Separated Molten Pool

Considering the issues arising from hybrid laser/GTAW in a common molten pool, a welding procedure based on using leading GTAW as an auxiliary preheating source followed by a fiber laser beam as a main heat source is developed to join galvanized dual-phase (DP) 980 steel in a gap-free lap joint configuration. The laser beam is separated from the GTAW torch at a specific distance to create two separate molten pools. It should be mentioned that the specific distance between the laser beam and GTAW torch depends on the welding speed and laser power used as well as the other welding parameter settings. Figure 11 shows top, back, and cross-sectional views of the GTAW preheating weld. Figure 12 shows top, back, and cross-sectional views of the

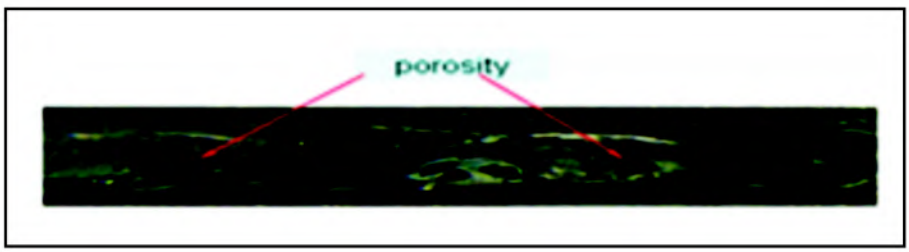

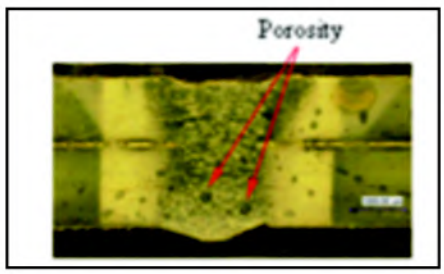

Fig. 9 — The formation of porosity in the welds produced by hybrid laser/GTAW in a common molten pool.

lap joint obtained by hybrid GTAW preheating/laser welding in a separated molten pool. As shown in Fig. 11A, after GTAW preheating, a thin layer of metal oxide film is produced at the top surface of the metal sheets with the specific heat input. In addition, a portion of the zinc coating in and around the weld zone at the interface of the two metal sheets is melted and the remnant zinc coating is oxidized, as shown in Fig. 11B. As mentioned previously, this zinc oxide can stabilize the welding process. Figure 12 shows that no spatter and porosity are produced in the surface of the weld. From Fig. 12C, it is observed that the weld is free from porosity. This suggests that a completely defect-free weld with complete penetration is obtained.

In this case, success in achieving completely defect-free welds is expected because of the formation of metal oxides produced by the GTAW preheating process. It is well known that for laser welding of steel or aluminum, most of the laser beam energy is reflected by the metal sheet surface (Ref. 41). In addition, when the welding process is under the keyhole mode the laser beam energy absorbed by the metal sheet can be significantly improved due to the multireflection function of the keyhole (Ref. 42). Furthermore, it was found that the presence of metal oxides (Refs. 41, 43) can significantly improve up to two to three times the absorption of laser beam energy. In this case, a thin film of metal oxide is produced during the GTAW preheating process with the controlled heat input welding condition. Due to the high transmittance and conductivity of zinc oxide and iron oxides, the coupling of laser beam energy into the specimen can be dramatically enhanced (Refs. 44, 45). Under this welding condition, the keyhole forms easily and keeps very stable, which provides the channel to vent out the highly pressurized zinc vapor developed at the interface of the two metal sheets. Consequently, the welding process can be stable. A CCD video camera is used to monitor the welding process and the dynamic behaviors of the molten pool online. By analyzing the film taken by the CCD video camera, it is found that when the keyhole is kept open, the welding process is very stable and a high-quality weld is achieved. However, when the keyhole collapses, the process becomes dramatically unstable and a weld is presented with the poor surface appearance and that is full of spatter and porosity. Figure 13 shows the open and the collapsed keyhole images. As shown in Fig. 13A, the black spot in the front of the molten pool presents the keyhole shape. A set of experiments is designed to verify that the absorption of laser beam energy by the metal sheets increases with the GTAW preheating process. The first test is performed with the removal of the zinc coating at the interface of the metal sheets; the second test is carried out with the zinc coating at the interface of two metal sheets while using GTAW to preheating the top surface of the metal sheets prior to the followed laser welding process. Laser power of 3000 W and a welding speed of 50 mm/s as well as the shielding gas rate of 30 ft^3/h are used in the first test. In the second test, the welding conditions were kept the same as in the first test, but an arc current of 300 A was used to preheating the metal sheet before the followed laser irradiated

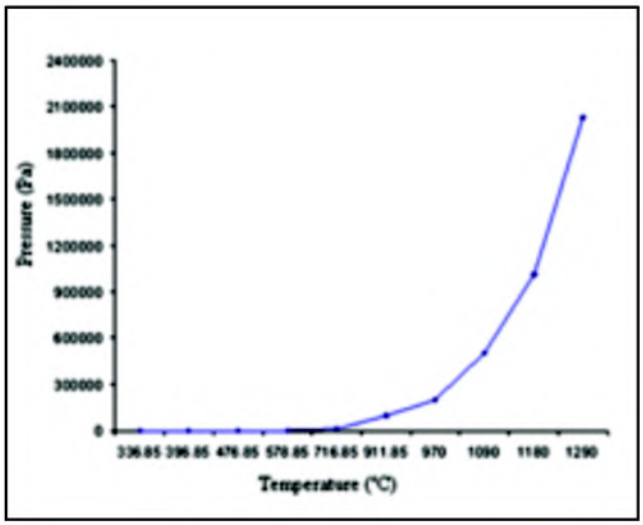

Fig. 10 — Relationship of the zinc pressure and temperature (Ref. 40).

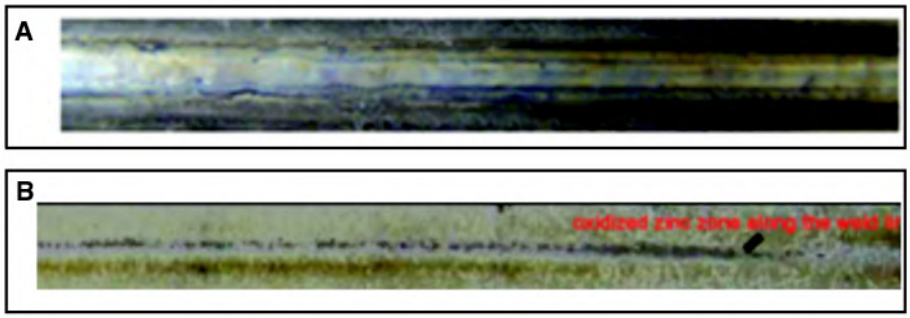

the metal sheets. As mentioned earlier, the pressure level of the highly pressurized zinc vapor is exponentially increased with the temperature. Additionally, when the laser beam is used on the focus, the width of the weld at the interface of the two metal sheets becomes very small at a welding speed of 50 mm/s, which decreases the weld strength. Furthermore, in order to maintain high productivity for industry, the GTAW torch preheating process should be kept synchronously with the followed laser beam welding process in practice. In order to produce the expected thin layer of metal oxides to enhance the coupling of laser beam energy into the welded materials, the GTAW preheating arc current should be increased when laser welding is increased, as mentioned before. The maximum arc current value that can be used is 300 A from the machine used in this study. When the laser welding speed is increased more than 50 mm/s, the 300-A GTAW preheating arc current fails to produce the thin layer of metal oxides required for improving the coupling of laser beam energy into the welded materials to generate the stable open keyhole to vent out the highly pressurized zinc vapor developed at the interface of the two metal sheets. Also, it is difficult to transform the zinc coating along the weld interface into the zinc oxides with the very high preheating speed at the current of 300 A. Considering these factors, the laser beam is defocused with a spot size of 1 mm in the previous two cases. Figure 14 shows the experimental results. As shown in Fig. 14B, the penetration depth of the laser welded joint obtained is as the function of the weld location. However, complete penetration is achieved in the second test, as shown in Fig. 14D. This fact confirms that surface modification of the preheating welding process significantly enhances absorption of laser beam energy.

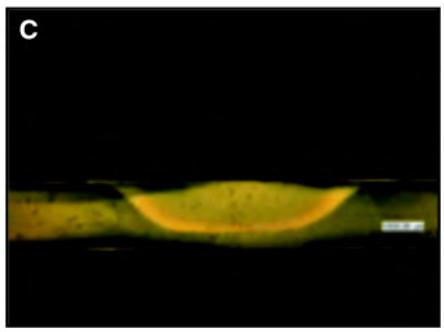

Fig. 11 — GTAW preheating weld with arc current 200 A: A — Top view of GTAW preheating weld B — back view of top metal sheet of GTAW preheating weld C — cross-sectional view of the GTA weld. (Arc current: 200A, the tip distance of electrode with respect to the top surface of the metal sheets: 3 mm, and welding speed: 30 mm/s.)

X-ray photoelectron spectroscopy (XPS) tests are also carried out to analyze

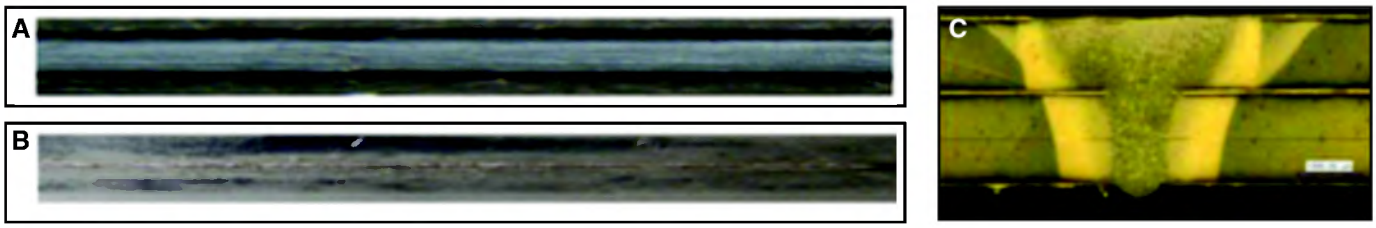

Fig. 12 — Views of the hybrid laser-GTAW preheating joint: A — Top view; B — back view; C — cross-sectional view. (Laser power: 3000 W, arc current: 200 A, and welding speed: 30 mm/s.)

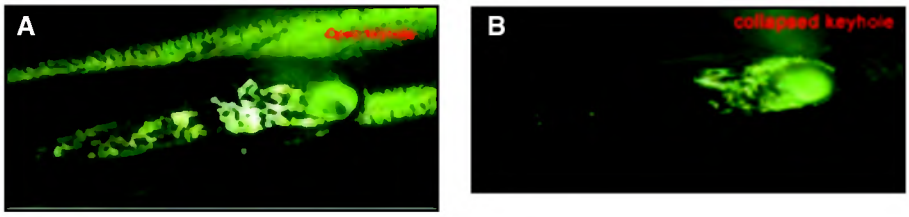

Fig. 13 — A — Opening of the keyhole; B — collapse of the keyhole.

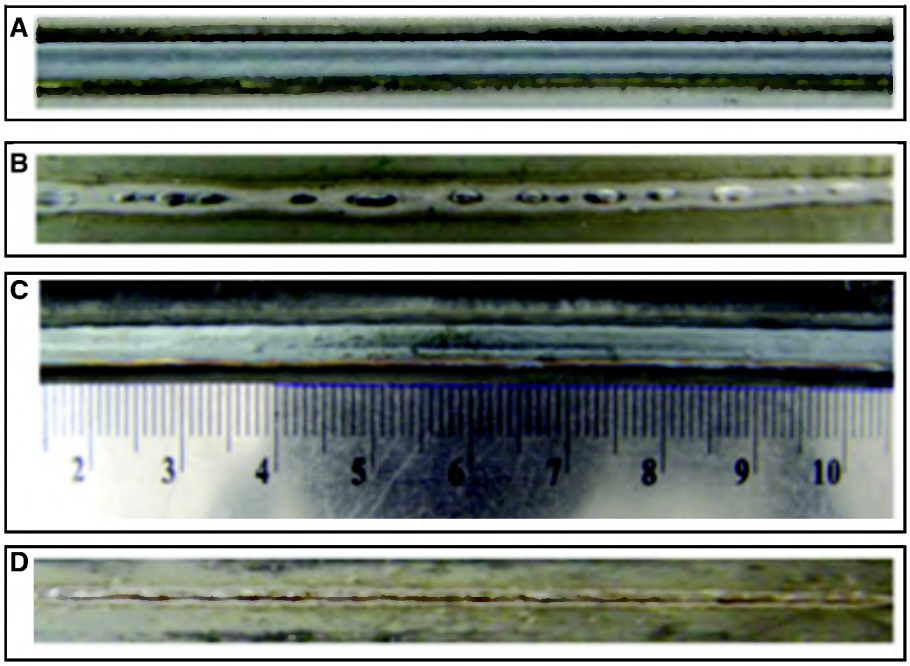

Fig. 14 — Comparison of the weld depth penetration in different welding conditions: A — Top view of laser weld without the zinc coating at the interface of two metal sheets; B — back view of laser weld without the zinc coating at the interface of two metal sheets; C — top view of hybrid laser-GTAW preheating weld with the zinc coating at the interface of two metal sheets; D — back view of hybrid laser-GTAW preheating weld with the zinc coating at the interface of two metal sheets. (Laser power of 3000 W and welding speed of 50 mm/s for A and B; laser power of 3000 W, preheating arc current of 300 A, GTAW preheating welding speed of 50 mm/s, and laser welding speed of 50 mm/s for C and D.)

the chemical compositions of the GTAW preheating weld to confirm the above speculation of the formation of metal oxides during the GTAW preheating process. The sample of the GTAW preheating weld for the XPS analysis is obtained with an arc preheating current of 200 A, welding speed of 30 mm/s, and shielding gas flow rate of 30 ft^3/h. The distance between the tip and the top surface of the metal sheets is 3 mm. The elemental identification can be made by comparing the peak binding energies obtained through XPS analysis to the tabulated values. As shown in Fig. 15B, there are two strong peaks located at 530.8 eV and 1022.3 eV due to the O(1s) and Zn (2p3) binding energy of zinc oxides. This value of Zn2p3 in this study (1022.4 eV) is good agreement with those for ZnO (1022.3 eV) reported in the literature (Refs. 46, 47). It indicates that zinc oxide is formed at the top surface and the interface. The proportion of C1s, O1s, Zn2P3, and Ca2P for the GTAW preheating welds were presented in the Atomic Concentration Table shown in Fig. 15B on the basis of the relative area under the specific element peaks. Additionally, when the laser beam is in the separated molten pool with the electrode torch, the coupling of laser beam energy into the metal sheets is free from the influence of arc plasma and laser-induced zinc plume which occur in the hybrid laser/GTA welding in the common molten pool. Furthermore, it is found that when the GTAW preheating arc current below some level the metal oxides could not be formed and only the soot was generated at the top surface.

During the GTAW preheating process, the zinc oxides have priority to be formed over the iron oxides because the zinc coating at the top surface of the metal sheets is first under the heat from the GTAW preheating. Once the zinc oxide is formed at the top surface, it inhibits formation of iron oxides. Before the zinc oxides decompose, it is difficult to produce the iron oxides. Due to the high temperature under the arc, the zinc oxides are generally unstable and susceptible to immediately decomposing. Under this welding condition, the top surface of the metal sheet melts and iron oxides are formed at the top surface of the metal sheets presented in Fig. 16A, which also can enhance the absorption of laser beam and help facilitate the formation of the keyhole. As shown in Fig. 16B, a sound weld is still obtained. As the GTAW preheating arc current keeps increasing, iron oxides are also completely decomposed. Once the preheating arc current reaches some kind of high level, different kinds of humping are present in the surface of the preheating welds, as shown in Fig. 16C. It should be mentioned that chemical compositions produced by the GTAW preheating process are sensitive to the GTAW preheating welding parameters such as the preheating arc current, the distance between the tip of the GTAW electrode tip and the top surface of two metal sheets, and the shielding gas rate. A change in any of the welding parameters mentioned above results in different surface conditions. It is also necessary to point out that the distance between the laser beam and the electrode is required to be long enough to lower the pressure level of the zinc vapor at the interface of two metal sheets to some extent. In this case, the distance is kept at 190 mm. Further study of the relationship between the pressure level of the developed highly pressurized zinc vapor at the interface of two metal sheets and the different welding parameters is important

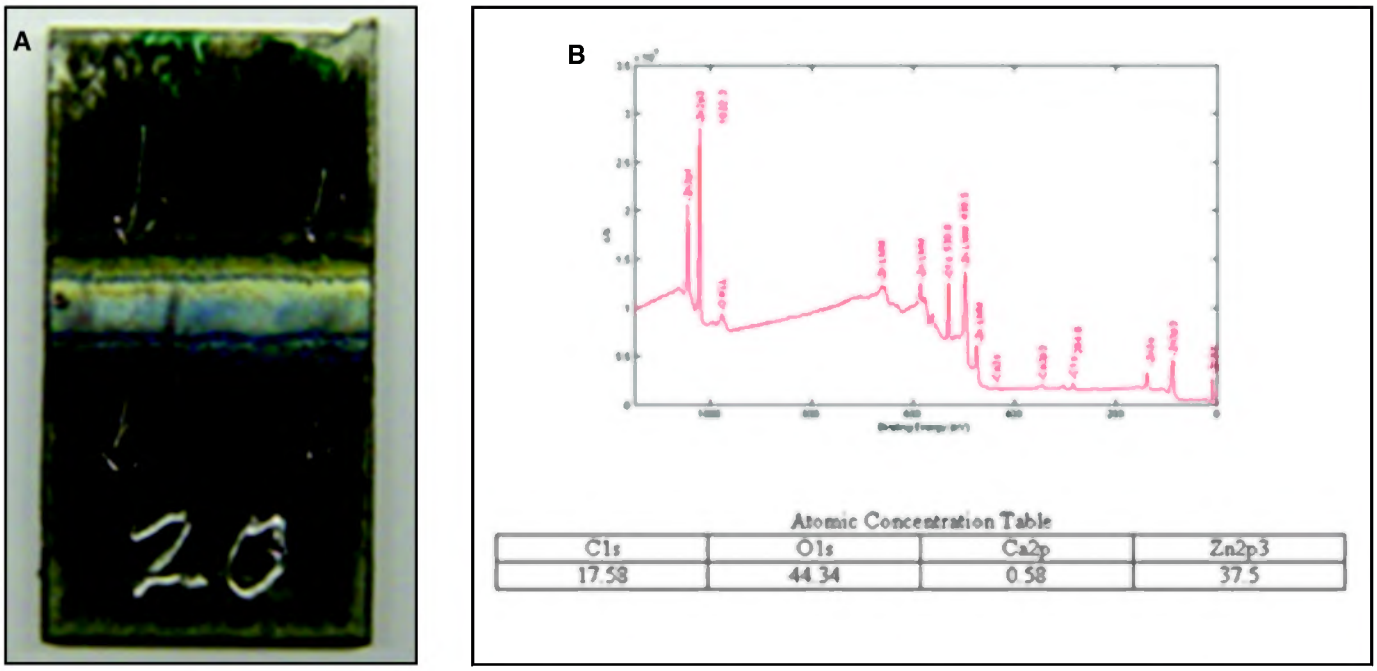

Fig. 15 — The XPS analysis results of the heated surface of DP 980 galvanized steel by GTAW torch: A — The measured points; B — XPS analysis results.

and required. Additionally, the distance between the laser beam and the electrode can be shortened with the assistance of using the copper block as the welding support platform or water cooling system.

For $Zn + 1/2O_2 \rightarrow ZnO$, the molecular weight of ZnO is 81.4084 *mol/L* and that of Zn is 65.38 *mol/L*. The density of zinc is 7.133 g/cm^3 and the density of zinc oxide is 5.606 g/cm^3 (Ref. 40). The rate at which the zinc oxide occurs during the GTAW preheating process can be calculated by the Pilling-Bedworth (PB) ratio equation (Ref. 48):

$$P-B=\frac{M_{ZnO}\,\rho_{Zn}}{M_{Zn}\rho_{ZnO}}=\frac{\left(81.4084\frac{gm}{mol}\right)\left(7.133g/cm^3\right)}{\left(65.38\frac{gm}{mol}\right)\left(5.606g/cm^3\right)}=1.584$$

The P-B ratio of ZnO oxide indicates that the volumes of the zinc oxide and the transformed zinc coating are similar and "an adherent, nonporous, and protective" zinc film is produced at the top surface during the GTAW preheating process (Ref. 48).

Microhardness Measurement, SEM Analysis, and Failure Analysis for the Hybrid GTAW Preheating/Laser Welded Joints in the Separated Molten Pool

Vickers microhardness measurement is preformed along the weld fusion zone and heat-affected zone (HAZ) for the hybrid GTAW preheating/laser welded joint. The indenter load used in the microhardness test is 200 g. The impressions are made in the increment of 0.25 mm away from the interface of the two metal sheets. Figure 17 shows the typical microhardness features of the welded joint obtained by the hybrid GTAW preheating/laser welding process in the separated molten pool with a laser power of 3 kW, GTAW preheating arc current of 200 A, and welding speed of 30 mm/s. As shown in Fig. 17, the hardness distribution is not uniform along the weld. After showing a relatively uniform value in the weld zone, the hardness value decreased continuously to the minimum value in the HAZ away from the weld zone toward the HAZ, and then gradually increased again in the base material. The maximum hardness value (393.5 HV) is located at the center of the weld. The minimum hardness value (200.6 HV) is found in the HAZ. As shown in Fig. 17, the HAZ has a lower hardness value than that in the base material and the welded zone, which indicates that the HAZ is softened. The degradation of the hardness in the HAZ has a weakening effect on the mechanical structure of the joint. Additionally, SEM analysis of the microstructure was also performed at selected locations in the cross section, as shown in Fig. 18A–F.

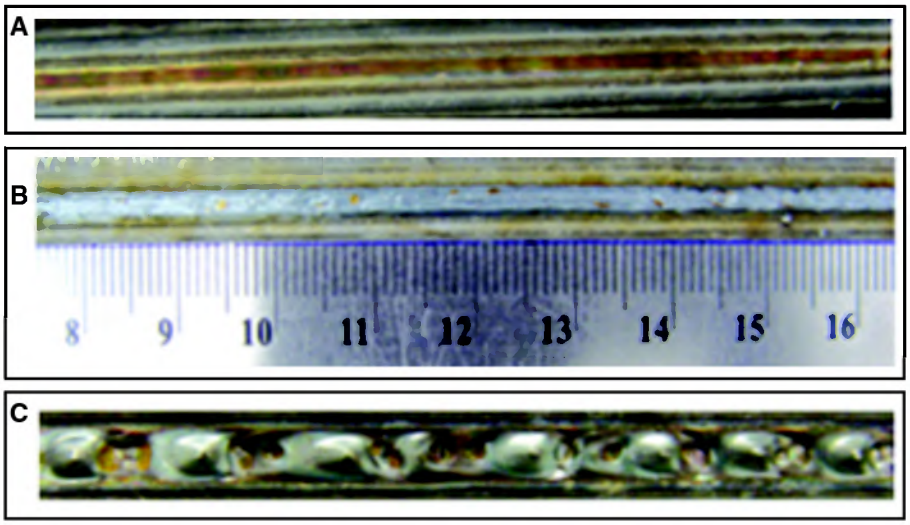

Fig. 16 — A — Top view of the preheating weld with the iron oxide film at the arc current of 230 A; B — top view of hybrid GTAW preheating/ laser welding with a separated molten pool; C — the humping produced in the GTAW preheating weld at an arc current of 240 A (welding speed: 30 mm/s; distance between the electrode tip and the top surface of two metal sheets: 3 mm; shielding gas flow rate: 30 ft³/h).

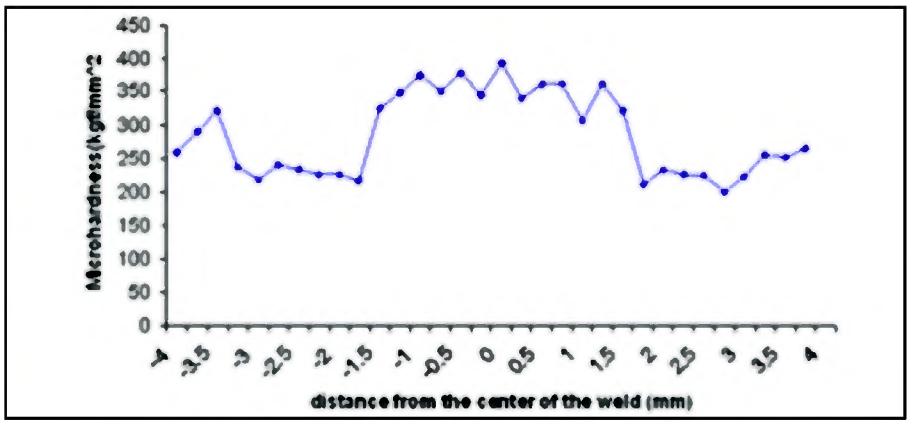

Fig. 17 — Microhardness distribution of the welded joint obtained by hybrid GTAW preheating/laser welding in the separated molten pool.

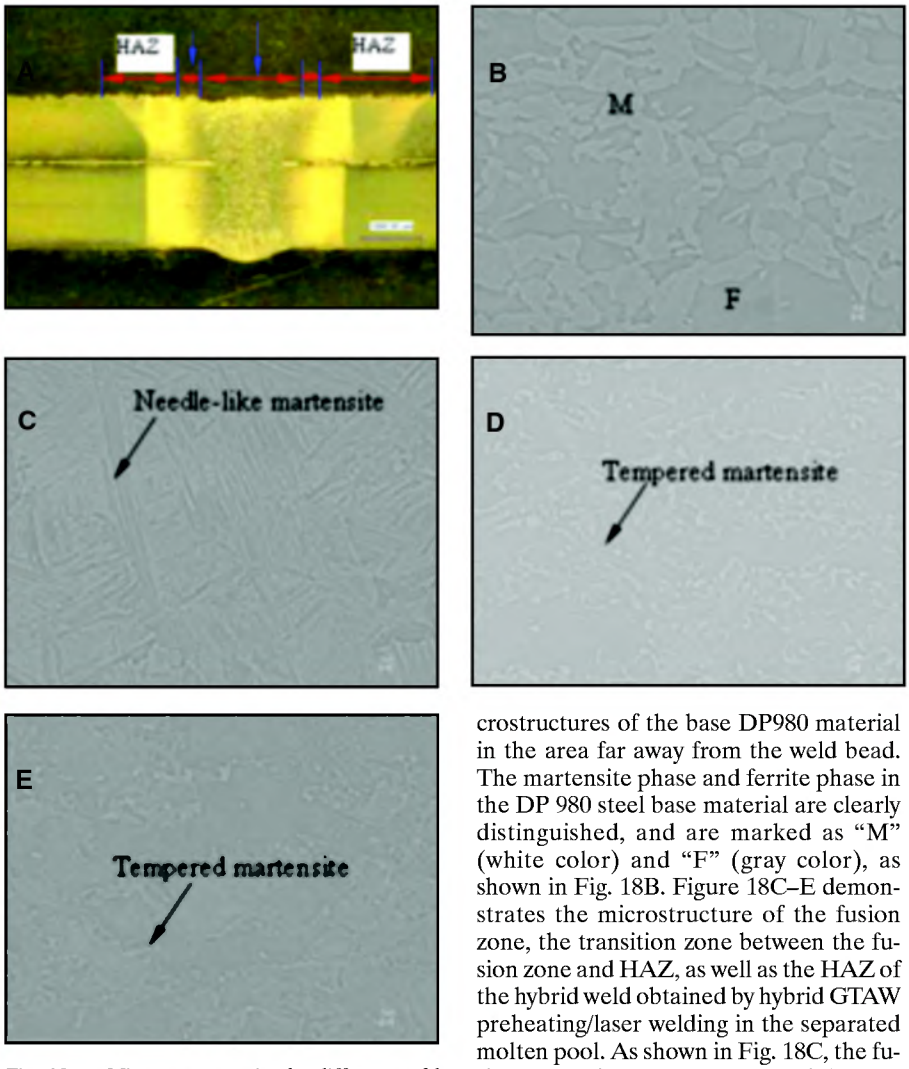

Fig. 18 — Microstructures in the different weld zones: A — Cross-sectional view of the weld; B — in the base material; C — in the fusion zone; D — in the transitional region between the fusion zone and HAZ; E — in the HAZ.

Figure 18A shows the cross-sectional view of the hybrid GTAW preheating/laser welded joint. Figure 18B shows the microstructures of the base DP980 material in the area far away from the weld bead. The martensite phase and ferrite phase in the DP 980 steel base material are clearly distinguished, and are marked as "M" (white color) and "F" (gray color), as shown in Fig. 18B. Figure 18C–E demonstrates the microstructure of the fusion zone, the transition zone between the fusion zone and HAZ, as well as the HAZ of the hybrid weld obtained by hybrid GTAW preheating/laser welding in the separated molten pool. As shown in Fig. 18C, the fusion zone microstructure was mainly composed of tempered martensite and ferrite. Compared to the volume of martensite in the base material and the weld zone, the volume of martensite in the transition between the weld zone and HAZ is decreased, as shown in Fig. 18D. Furthermore, it is obvious that the volume of martensite in the HAZ, as shown in Fig. 18E, is dramatically decreased compared to that in the base material, fusion zone, and transition zone between the fusion zone and HAZ of the hybrid weld. This is the reason why the hardness in the HAZ of the hybrid weld is dramatically degraded.

Tensile shear tests were also performed to assess the strength of the welds. Figure 19 shows the tensile shear test specimen dimensions and the fracture location of the welds when applying the loads during the tensile shear tests. From the test results, it is found that all of the specimens broke in the HAZ instead of in the base material, as shown in Fig. 20. Only two specimens broke in the fusion zone of welds made at a welding speed of 50 mm/s and laser power of 3 kW as well as a preheating arc current of 200 A. The tensile shear test results confirmed that the HAZ is softened during the welding process.

Conclusions

In order to weld galvanized DP 980 steel in a gap-free lap joint configuration, a hybrid laser/GTA welding technique is accomplished in two modes: 1) The laser beam shares a common molten pool with the electrode; and 2) the laser beam and the electrode produced two separated molten pools and the GTAW is only used for the surface modification. The results obtained from this study are as follows:

1) Compared to laser welding of galvanized DP 980 steel in a gap-free lap joint configuration, the introduction of arc in hybrid laser-arc welding process when the laser and arc share a common molten pool can suppress the formation of spatter to some extent. In addition, the stability of the welding process is enhanced with the increase in the arc current in the specific range and distance between the laser beam and the GTAW torch.

2) When the laser beam and the GTAW torch share a common molten pool, the coupling of laser beam energy and arc plasma significantly fluctuates over time and the welding process is unstable, which results in different weld defects such as spatter and porosity.

3) When the air or metal vapor is entrapped into the molten pool and cannot escape from it during the solidification process, external or internal porosity is formed in the weld.

4) Completely defect-free welds are obtained by the GTAW preheating/laser welding procedure in the separated molten pool where the GTAW is only used to preheat the metal sheets to modify the surface conditions. Chemical compositions of the top surface of two metal sheets produced by the GTAW preheating welding process are sensitive to the GTAW preheating welding conditions. Different metal oxides are produced with various preheating welding

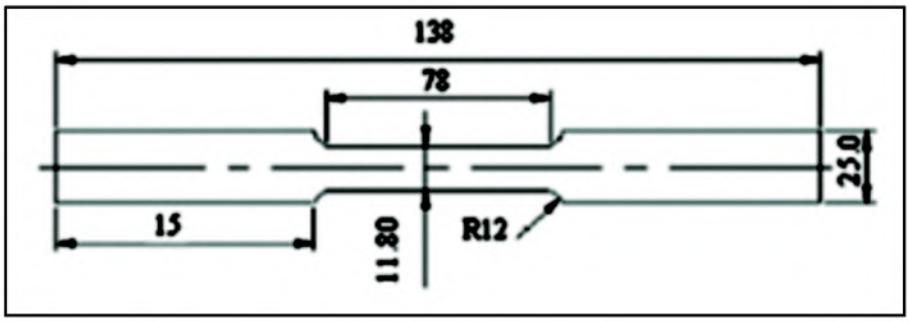

Fig. 19 — Schematic presentation of the tensile shear test specimen.

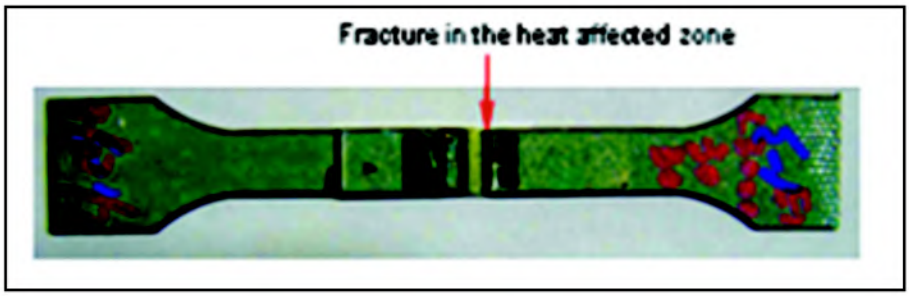

Fig. 20 — Fracture in the HAZ.

conditions. Compared to laser welding without GTAW preheating, these metal oxides can dramatically improve the coupling efficiency of the laser beam energy into the metal sheets by two or more times to generate the keyhole, which provides the channel for the highly pressurized zinc vapor developed at the interface of two metal sheets to be vented out. Thus, the welding process is stable and the welding speed can be significantly increased.

5) Under the specific GTAW preheating welding conditions, a portion of the zinc coating at the interface of two metal sheets melts and a portion of the zinc coating oxidizes. The zinc oxides have a higher melting point (1975°C) than the boiling point of zinc, which helps to stabilize the following welding process and lower the pressure level of the zinc vapor for the following laser welding process. The XPS analysis results confirm this fact. In addition, there is a minimum requirement of the distance between laser beam and electrode torch, which can be shortened with the assistance of a cooling system.

6) When the keyhole is kept open, the welding process is stable. However, the keyhole tends to collapse, and the welding process becomes unstable. Consequently, maintaining the opening of the keyhole is the critical factor to guarantee the achievement of sound welds.

7) The heat-affected zone is softened due to the decrease in the volume fraction of martensite. Due to the softening effect, the lowest microhardness value is obtained in the HAZ and the specimens broke in the HAZ during the tensile shear tests.

Acknowledgments

The authors gratefully acknowledge financial support from General Motors and National Science Foundation with grant number EEC-0541952. They would also like to thank Dechao Lin and Andrew Socha, research engineers at SMU's Research Center for Advanced Manufacturing for assisting in the experimental setup. Thanks should also be given to Wei Huang and Fanrong Kong, PhD candidates at SMU's Research Center for Advanced Manufacturing, for help with the experiments.

References

1. Akhter, R., Steen, W. M., and Watkins, K. G. 1991. Welding zinc-coated steel with a laser and the properties of the weldment. *Journal of Laser Applications* 3(2): 9–20.

2. AWS WZC/D19.0-72, *Welding Zinc-Coated Steels*. 1972. Miami, Fla.: American Welding Society.

3. Graham, M. P., Hirak, D. M., Kerr, H. W., and Weckman, D. C. 1994. Nd:YAG laser welding of coated sheet steel. *Journal of Laser Applications* 6(4): 212–222.

4. Mazumder, J., Dasgupta, A., and Bembenek, M. 2002. Alloy based laser welding. U.S. Patent 6,479,168.

5. Dasgupta, A., Mazumder, J., and Bembenek, M. 2000. Alloying based laser welding of galvanized steel. *Proceedings of International Conference on Applications of Lasers and Electro-Optics*. Laser Institute of America, Dearborn, Mich.

6. Dasgupta, A., and Mazumder, J. 2006. A novel method for lap welding of automotive sheet steel using high power CW CO_2 laser. *Proceedings of the 4th International Congress on Laser Advanced Materials Processing.*

7. Pieters, R. R. G. M., Bakels, J. G., Hermans, M. J. M., and den Ouden, G. 2006. Laser welding of zinc coated steels in an edge lap configuration. *Journal of Laser Applications* 18(3): 199–204.

8. Graham, M. P., Hirak, D. M., Kerr, H. W., and Weckman, D. C. 1994. Nd:YAG laser welding of coated sheet steel. *Journal of Laser Applications* 6(4): 212–222.

9. Sacks, J. L., Davis, H., and Spilchen, W. 2007. Corrosion resistant wire products and method of making same. U.S. Patent 20070119715.

10. Graham, M. P., Hirak, D. M., Kerr, H. W., and Weckman, D. C. 1996. Nd:YAG laser beam welding of coated steels using a modified lap joint geometry. *Welding Journal* 75(5): 162-s to 170-s.

11. Graham, M. P., Hirak, D. M., Kerr, H. W., and Weckman, D. C. 1996. Laser welding of Zn-coated sheet steels. *Proceeding of SPIE: International Society for Optical Engineering*, Vol. 2703.

12. Pennington, E. J. 1987. Laser welding of galvanized steel. U.S. Patent No. 4642446.

13. Williams, S. W., Salter, P. L., Scott, G., and Harris, S. J. 1993. New welding process for galvanized steel. *Proc. 26th Int. Symp. Automotive Technology and Automation*, Aachen, Germany. pp. 49–56.

14. Tzeng, Y. F. 1999. Pulsed Nd:YAG laser seam welding of zinc-coated steel. *Welding Journal* 78(7): 238-s to 244-s.

15. Forrest, M. G., and Lu, F. 2005. Development of an advanced dual beam head for laser lap joining of zinc coated steel sheet without gap at the interface. *24th International Congress on Applications of Lasers and Electro-Optics* (ICALEO) pp. 1069–1074.

16. Forrest, M. G., and Lu, F. 2003. Fundamental study of dual beam laser welding of zinc coated steel sheets without gap at the interface. *ICALEO 2003 International Congress on Applications of Lasers and Electro-Optics*, Jacksonville, Fla.

17. Xie, J. 2002. Dual beam laser welding. *Welding Journal* 81(10): 223-s to 230-s.

18. Gualini, M. M. S., Iqbal, S., and Grassi, F. 2006. Modified dual-beam method for welding galvanized steel sheets in lap configuration. *Journal of Laser Applications* 18(3): 185–191.

19. Forrest, M. G., and Lu, F. 2005. Development of an advanced dual beam head for laser lap joining of zinc coated steel sheet without gap at the interface. *24th International Congress on Applications of Lasers and Electro-Optics,* pp. 1069–1074.

20. Choi, H. W., Farson, D. F., and Cho, M. H. 2006. Using a hybrid laser plus GMAW process for controlling the bead humping defect. *Welding Journal* 85(8) :174-s to 179-s.

21. Mueller, G. H. 2004. Hybrid welding of galvanized steel sheet. European patent EP 1454701.

22. Kusch, M., and Thurner, S. 2008. Application of the plasma-MIG technology for the joining of galvanized steel materials. *Welding and Cutting* 7(1): 54–59.

23. Kim, C., Choi, W., Kim, J., and Rhee, S. 2008. Relationship between the weldability and the process parameters for laser-TIG hybrid welding of galvanized steel sheets. *Materials Transactions* 49(1): 179–186.

24. Gu, H., and Mueller, R. 2001. Hybrid welding of galvanized steel sheet. *20th International Congress on Applications of Lasers & Electro-optics (ICALEO)*, pp. 13–19.

25. Li, X. G., Lawson, W. H. S., and Zhou, Y. N. 2008. Lap welding of steel articles having a corrosion resisting metallic coating. U.S. Patent 2008/0035615 A1.

26. Li, X., Lawson, S., and Zhou, Y. 2007. Novel technique for laser lap welding of zinc coated sheet steels. *Journal of Laser Applications* 19(4): 259–264.

27. Nath, A. K., Sridhar, R., Ganesh, P., and Kaul, R. 2002. Laser power coupling efficiency in conduction and keyhole welding of austenitic stainless steel. *Sādhanā* 27: 383–392.

28. Arata, Y., and Miyamato, I. 1972. Some fundamental properties of high power laser beam as a heat source (report 2). *Transaction of Japan Welding Society* 3(1): 152–162.

29. Patel, R. S., and Brewster, M. Q. 1990. Effect of oxidation and plume formation on low power Nd:YAG laser metal interaction. *Journal of Heat Transfer, Transaction of ASME* 112(1): 170–177.

30. Zhu, X. D., Ma, Z. H., and Wang, L. Current status of advanced high-strength steel for auto-making and its development in Baosteel. At *www.baosteel.com*.

31. Materials selected for ULSAB-AVC. Online at *www.worldautosteel.org*.

32. Duley, W. W. 1998. Laser welding. Wiley-Interscience Press.

33. Davies, G. 2004. *Materials for Automobile Bodies* (1st edition). Butterworth-Heinemann.

34. Xie, J. 1999. Plasma fluctuation and keyhole instability in laser welding. *International Conference on Applications of Laser and Electro-Optics (ICALEO'99)*. P. Christensen, editor. San Diego, Calif.

35. Xie, J. 2002. Dual beam laser welding. *Welding Journal* 81(10): 223-s to 230-s.

36. Zhang, Y. M., and Zhang, S. B. 1999. Observation of the keyhole during plasma arc welding. *Welding Journal* 78(2): 53-s to 58-s.

37. Sibillano, T., Ancona, A., Berardi, V., Schingaro, E., Basile, G., and Lugarà, P. M. 2007. Optical detection of conduction/keyhole mode transition in laser welding. *Journal of Material Processing Technology* 191(1–3): 364–367.

38. Wang, H. X., and Chen, X. 2003. Three-dimensional modeling of the laser-induced plasma plume characteristics in laser welding. *Journal Physics D: Applied Physics* 36: 628–639.

39. Naito, Y., Katayama, S., and Matsunawa, A. 2003. Keyhole behavior and liquid flow in molten pool during laser-arc hybrid welding. *Proc. SPIE* Vol. 4831: 357–362.

40. Shackelford, J. F., and Alexander, W. 2000. *Materials Science and Engineering Handbook* (3rd edition), CRC Press.

41. Xie, J., and Kar, A. 1999. Laser welding of thin sheet steel with surface oxidation. *Welding Journal* 78(10): 343-s to 348-s.

42. Silfvast, W. T. 1996. *Laser Fundamentals*. Cambridge University Press.

43. Duley, W. W. 1999. *Laser Welding*. Toronto, Canada: Wiley Interscience.

44. Fang, Z. B., Tan, Y. S., Gong, H. X., Zhen, C. M., He, Z. W., and Wang, Y. Y. 2005. Transparent conductive Tb-doped ZnO films prepared by rf reactive magnetron sputtering. *Materials Letters* 59(21): 2611–2614.

45. Nickel, N. H., and Terukov, E. 2004. *Zinc Oxide — A Material for Micro- and Optoelectronic Applications*. Springer Press.

46. Briggs, D. 1988. *Handbook of X-ray and Ultraviolet Photoelectron Spectroscopy*. Heydin Press.

47. Wagner, C. D. 1991. The NIST X-ray photoelectron spectroscopy (XPS) database microform. NIST technical note.

48. Askeland, D. R., and Phulé, P. P. 2006. *The Science and Engineering of Materials* (5th edition). Thomson Press.

Preparation of Manuscripts for Submission to the *Welding Journal* Research Supplement

All authors should address themselves to the following questions when writing papers for submission to the Welding Research Supplement:

- Why was the work done?
- What was done?
- What was found?
- What is the significance of your results?
- What are your most important conclusions?

With those questions in mind, most authors can logically organize their material along the following lines, using suitable headings and subheadings to divide the paper.

1) **Abstract.** A concise summary of the major elements of the presentation, not exceeding 200 words, to help the reader decide if the information is for him or her.

2) **Introduction.** A short statement giving relevant background, purpose, and scope to help orient the reader. Do not duplicate the abstract.

3) **Experimental Procedure, Materials, Equipment.**

4) **Results, Discussion.** The facts or data obtained and their evaluation.

5) **Conclusion.** An evaluation and interpretation of your results. Most often, this is what the readers remember.

6) **Acknowledgment, References and Appendix.**

Keep in mind that proper use of terms, abbreviations, and symbols are important considerations in processing a manuscript for publication. For welding terminology, the *Welding Journal* adheres to AWS A3.0:2001, *Standard Welding Terms and Definitions*.

Papers submitted for consideration in the Welding Research Supplement are required to undergo Peer Review before acceptance for publication. Submit an original and one copy (double-spaced, with 1-in. margins on 8 ½ x 11-in. or A4 paper) of the manuscript. A manuscript submission form should accompany the manuscript.

Tables and figures should be separate from the manuscript copy and only high-quality figures will be published. Figures should be original line art or glossy photos. Special instructions are required if figures are submitted by electronic means. To receive complete instructions and the manuscript submission form, please contact the Peer Review Coordinator, Erin Adams, at (305) 443-9353, ext. 275; FAX 305-443-7404; or write to the American Welding Society, 550 NW LeJeune Rd., Miami, FL 33126.